Volume 252, No. 8, 15 February 2006 ISSN 0169-4332

Available online at www.sciencedirect.com
SCIENCE DIRECT
Applied Surface Science 252 (2006) 2826–2831
applied surface science
www.elsevier.com/locate/apsusc

Photoluminescence of thermal-annealed nanocolumnar ZnO thin films grown by electrodeposition

B. Marí [a,*], F.J. Manjón [a], M. Mollar [a], J. Cembrero [b], R. Gómez [c]

[a] *Departament de Física Aplicada, Universitat Politècnica de València, Camí de Vera s/n, 46022 València, Spain*
[b] *Departament d'Enginyeria Mecànica i Materials, Universitat Politècnica de València, Camí de Vera s/n, 46022 València, Spain*
[c] *Departament de Química Física i Institut Universitari d'Electroquímica, Universitat d'Alacant, Ap. 99, E-03080 Alacant, Spain*

Received 11 January 2005; received in revised form 19 April 2005; accepted 19 April 2005
Available online 3 June 2005

Abstract

Nanostructured zinc oxide thin films formed by partially oriented hexagonal columns with dimensions of about 100 nm × 300 nm have been prepared by cathodic electrodeposition on conducting glass substrates. After subsequent thermal annealing in air at different temperatures (100–500 °C), structural information on the films was obtained by means of non-resonant Raman spectroscopy. Increasing the annealing temperature leads to a higher degree of crystallinity. The photoluminescence activity of the samples (at low temperature) also improves for increasing annealing temperatures in two ways: increasing the intensity of the near-band edge emission and decreasing the width of the excitonic peak. No emission band in the visible is detected, which attests the high quality of the ZnO nanocolumnar films.

Keywords: ZnO; Photoluminescence; Nanostructures; Electrodeposition; Transparent conducting oxide

1. Introduction

Nanostructured materials are attracting an increasing interest, and even excitement, in nearly all fields of science and technology owing to their potential applications and to the appearance of phenomena and properties different from those of the corresponding bulk phases. In particular, nanostructured semiconductor materials have drawn much attention due to their unique physical, chemical and optical properties. These nanoscaled structures underlie the development of new devices based on mixed or interpenetrated materials. For instance, nanostructured solar cells constituted by absorbers with thicknesses of a few nanometres and active interfaces coated with very thin insulating oxides have been recently proposed as to improve device performance [1,2]. Understanding the effects of size and dimensionality on properties is facilitated by the synthesis and characterization of one-dimensional nanoscale materials (i.e., nanorods, nanowires, nanobelts, etc.). In addition, these materials have a

* Corresponding author. Tel.: +34 963 877 525; fax: +34 963 877 189.
E-mail address: bmari@fis.upv.es (B. Marí).

0169-4332/$ – see front matter © 2005 Elsevier B.V. All rights reserved.
doi:10.1016/j.apsusc.2005.04.024

potential application in constructing nanoscale electronic and optoelectronic devices.

Conversely, zinc oxide (ZnO) is an interesting semiconductor with a direct band gap of around 3.3 eV at room temperature and large exciton binding energy (60 meV). It is an important material in various fields of applications, being used as varistors, phosphors, piezoelectric transducers and transparent conducting films [3]. Additionally, in the last few years, owing to its potential applications in ultraviolet optoelectronic devices, zinc oxide has been the object of a quickly growing number of research projects.

Various methods have been employed in the synthesis of nanosized ZnO samples: spray pyrolysis, precipitation, thermal decomposition, hydrothermal synthesis, metal-organic vapor-phase epitaxial growth, etc. Recently it has been shown that this material can be also grown in nanostructured films (nanopillars) in a highly reproducible way by means of (epitaxial) electrodeposition (ED). This technique allows the dimensions of the nanostructures to be easily controlled by means of the growth parameters [4]. Moreover, the nanostructured ZnO samples obtained by ED exhibit good luminescent properties and are suitable structures to be used as host material in nanostructured solar cells [5]. It is also worth noting that electrodeposition is an efficient scalable nanotechnology, which can be used to produce highly structured nanoscale ZnO films at a reduced cost.

In this paper we have characterized the crystal quality of nanostructured ZnO films grown by electrodeposition (ED) by means of Raman spectroscopy and we have investigated how an improvement in the ZnO nanocrystals quality influences the luminescent properties of the films.

2. Experimental

The electrodeposition procedure involves a classical three electrode electrochemical setup (potentiostat/galvanostat) and a solution containing 5×10^{-3} M $ZnCl_2$, 10^{-1} M KCl and dissolved oxygen in deionized water. A Pt counter electrode and Ag/AgCl reference electrode were employed. The ED process was performed onto glass coated with a F-doped SnO_2 thin film (working electrode). Three growth variables were controlled during ED: current density, deposition time and temperature of the working electrolyte. In the present case, samples were prepared under a current density of 2.5 mA/cm^2 maintained for 30 min at a relatively low temperature of 65 °C. The ZnO films synthesized in this way are formed by nanocolumns with perfect hexagonal end planes of average diameter of about 100 nm and well-faceted side surfaces about 300 nm long. After deposition the samples were annealed at 200, 300, 400 and 500 °C for 1 h in air atmosphere. It is remarkable that the thermal annealing process does not alter the morphology (size) of the nanocolumns.

Photoluminescence (PL) experiments were performed in backscattering geometry using for excitation a HeCd laser (325 nm) with an optical power of 30 mW. The emitted light was analyzed by a Jobin-Yvon HR460 spectrometer using a photomultiplier detector optimized for the UV range. Samples were mounted onto the cold finger of a He close cycle refrigerator and cooled down to the desired temperature.

Raman measurements have been performed under a backscattering geometry by using a LabRam microspectrometer (from Jovin-Yvon Horiba) with a resolution better than 3 cm^{-1}. Raman scattering spectra were obtained either with an Ar-ion laser at 514.5 nm or with a He–Ne laser at 632.8 nm. Both lasers were focused on the sample surface (thin film) into a ca. 2 μm spot. All the spectra are shown as obtained.

3. Results and discussion

3.1. Photoluminescence

Fig. 1 shows the PL spectrum of a ZnO sample annealed at 500 °C in air atmosphere. It is dominated by a strong ultraviolet feature corresponding to near-band-edge emission and associated to an exciton bounded to shallow donors. No luminescence was found in the visible. In particular the typical broad green emission appearing for wavelengths larger than ca. 500 nm is completely absent. The green emission has been associated to the presence of various point defects,

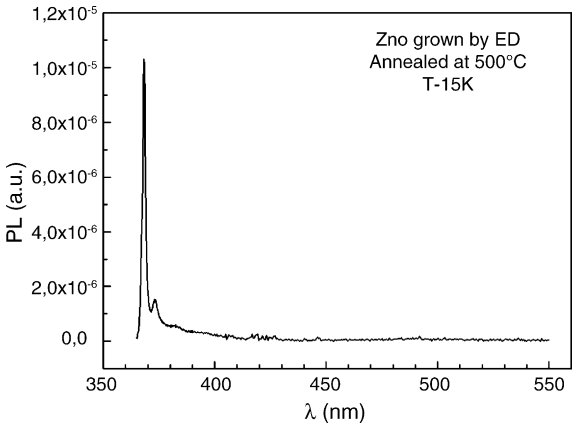

Fig. 1. Photoluminescence spectrum registered at 15 K of nanocolumnar ZnO crystals grown by ED and annealed at 500 °C.

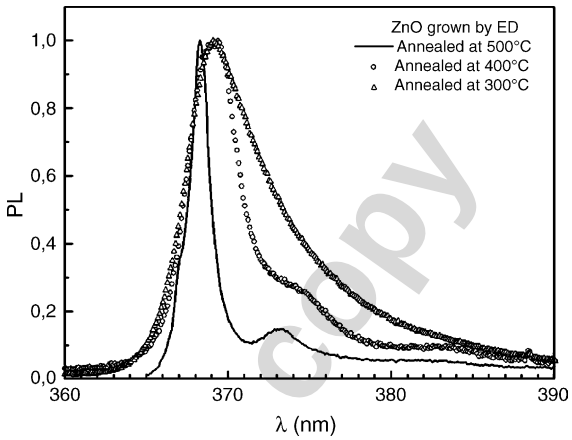

Fig. 2. Detail of the excitonic part of the photoluminescence for nanocolumnar ZnO crystals annealed at 300, 400 and 500 °C, respectively.

either extrinsic or intrinsic, which can easily form recombination centres. Most authors consider that these defects correspond to singly ionized oxygen vacancies [6,7]. Therefore, in our samples there is a very low concentration of such vacancies. A similar behaviour for nanorods with a diameter of ca. 100 nm and prepared by vapor-phase transport process has been reported [8].

It is worth noting that the thermal annealing triggers significant changes in the PL spectra: there is an increase in intensity and a narrowing of the main PL peak (not shown here) upon an increase in the annealing temperature. The fact that UV emission, mainly linked to the recombination of bound excitons, improves with the annealing temperature implies that the annealing decreases the concentration of non-radiative recombination centres, probably located at the surface of the nanocrystals. Of course, these non-radiative recombination centres would compete with the excitonic recombination, thus increasing the intensity of the UV emission.

Fig. 2 shows the detail of the PL spectra in the UV region as a function of the annealing temperature. The intensity of the PL peaks has been normalized in order to better appreciate the narrowing of the width of the peak as the annealing temperature increases. Interestingly, in the spectrum recorded after annealing at 500 °C the free exciton appears as a shoulder located at the side of higher energy of the main peak.

Two main characteristics have been observed in our PL spectrum: a narrowing and a blueshift of the main PL peak. We believe that the broad UV peak is from bound excitons related to an energy band associated to shallow donors. The narrowing of this peak is probably a consequence of the decrease of the width of this energy band. In non-intentionally doped ZnO samples there are two main shallow donors: H and Zn interstitials. Recent works have found that H diffuses from the ZnO lattice at temperatures higher than 600 °C [9]. On the other hand, the ZnO growth electrodeposition procedure, based on the contribution of incoming Zn ions in presence of oxygen, favours the excess of Zn in the ZnO lattice. The excess of Zn could be incorporated as interstitials or clusters. Since we have only reached annealing temperatures around 500 °C, we believe that the narrowing of the main PL peak in the UV is due to the diffusion of Zn interstitials from the ZnO lattice. Support for this conclusion is the fact that ZnO is ''radiation hard'' because of rapid defect annihilations [10]. This behaviour can be related to the high mobility of Zn ions in the ZnO lattice even at 150 K. That is, the annealing would induce ordering in the intrinsic defects, which would lead to a decrease of the number of non-radiative recombination centres and to a greater definition of the exciton-binding donor levels.

The main PL peak and the free exciton emission are blueshifted respect to ZnO bulk samples. The blueshift of this PL peak with increasing temperature can be accounted for by a compressive stress of the ZnO nanocolumns grown over FTO. Taking into account the bandgap shift with pressure (25 meV/GPa [11]) we estimate a compressive stress of 3 kbar in our samples.

3.2. Raman spectra

In order to follow the effect of the annealing process on the crystalline quality of the nanocolumns, we have performed non-resonant Raman scattering measurements at room temperature after annealing at different temperatures that are shown in Fig. 3. The spectra are shifted for the sake of clarity.

The Raman spectra of as-grown samples exhibit similar Raman spectra for nanocolumns with diameters ranging from 100 to 500 nm, i.e. no important size effects are found. However, the sample with the smaller column diameter shows a Raman spectrum with stronger features. In this case the Raman spectra depend in a remarkable way on the energy of excitation (see spectra (a) and (b) in Fig. 3). For excitation with the 632-nm laser (a) a stronger signal is evidenced in the acoustic region ranging from 0 to 300 cm^{-1} while for excitation with 514.5 nm (b) a stronger signal is observed in the optic range between 400 and 600 cm^{-1}. As already commented in Ref. [12], the Raman spectrum of the as-grown ZnO nanocrystals is characteristic of disordered or amorphous material and reflects the one-phonon density of states of wurtzite ZnO depicted in Fig. 2 after Ref. [13]. In fact, a small feature near 280 cm^{-1} can be observed in the Raman spectrum (a), which could be related to the silent B_1 (low) mode predicted to be near 261 cm^{-1} in Ref. [13]. This structure disappears with increasing the annealing temperature and has also been observed near 275 cm^{-1} in nanocrystalline ZnO thin films grown by rf sputtering [14,15]. The observation of the B_1 (low) mode could be likely due to the relaxation of the first-order selection rules in disordered materials or because of electric-field induced scattering in small nanocrystals as discussed in Refs [14,15]. The other silent mode (B_1 (high)), which could be observed in as-grown samples, is predicted to be around 550 cm^{-1} [13] near the A_1 (LO) mode and probably contributes to the observed feature of the one-phonon density of states near 550 cm^{-1} but cannot be identified in an isolated way.

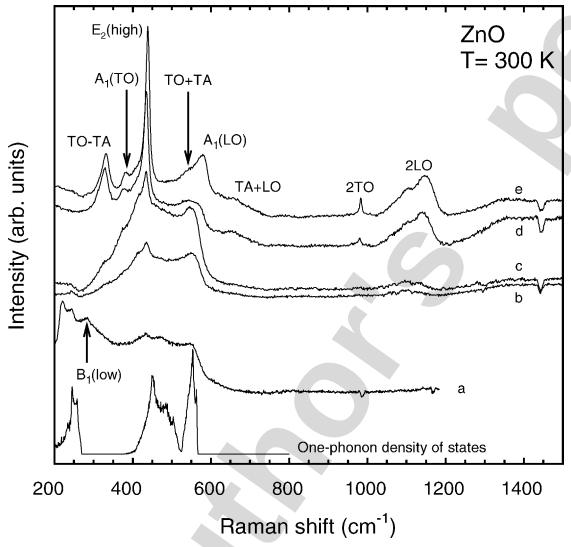

Fig. 3. Room-temperature Raman spectra of nanocolumnar ZnO crystals after annealing at different temperatures. (a) and (b) Raman spectra correspond to as-grown crystals excited with 632 and 514.5 nm, respectively. (c)–(e) Raman spectra correspond to excitation with 514.5 nm after annealing at 200, 400 and 500 °C, respectively. The calculated one-phonon density of states from first principles in Ref. [7] is also shown for comparison.

Raman spectra (c), (d) and (e) in Fig. 3 correspond to the same sample after annealing at 200, 400 and 500 °C respectively and excited with the Ar laser. Possible assignment for the different bands is also given. As mentioned above, ZnO crystals have a wurtzite structure. Group theory predicts that there are two A_1, two E_1, two E_2 and two B_1 modes (non-active). It can be observed that the broad band between 400 and 600 cm^{-1} corresponding to the one-phonon density of states disappears as the annealing temperature increases while the first-order modes appear in this region of the spectrum. Comparing the Raman spectra of the ZnO nanocolumnar crystals with that of the bulk, the Raman modes at 383, 438.5 and 575 cm^{-1} are assigned to A_1 (TO), E_2 (high) and A_1 (LO), respectively. It is interesting to note also that there is a feature at 982 cm^{-1} that develops with increasing the annealing temperature. It is possible that this feature corresponds to the enhanced 2TO feature [13] since several second order modes are clearly observed in the spectrum of the sample annealed at 500 °C; however, this attribution is somewhat doubtful because several works observed this mode at a similar frequency showing a much broader band [16–18].

The E_2 (high) mode is found at 438.5 cm^{-1} while in ZnO bulk samples is around 437 cm^{-1}. The shift of this mode and the other modes in the spectra annealed at 500 °C can be accounted for also by the compressive stress of the ZnO nanocolumns grown over FTO. Taking into account the shift with pressure

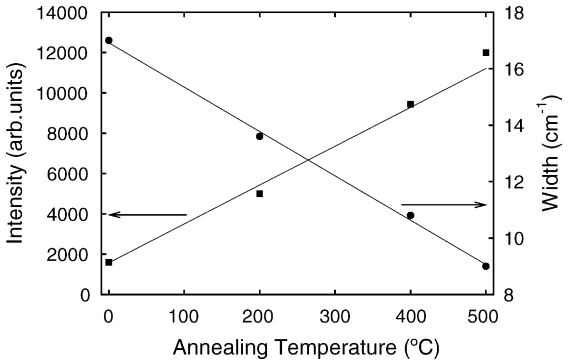

Fig. 4. Intensity and width (FWHM) of the E_2 (high) mode as a function of the annealing temperature.

(5.1 cm^{-1}/GPa [19]) we estimate a compressive stress of around 3 kbar in our samples. A similar compressive stress has been found in ZnO nanowires deposited over Si [20].

Fig. 4 shows the evolution of the intensity and width (FWHM) of the E_2 (high) mode after fitting the mode with a Voigt profile and substracting the resolution of the spectrometer. The intensity of the E_2 (high) mode increases linearly with increasing the annealing temperature up to 500 °C. The width of the E_2 (high) mode decreases also linearly with increasing the annealing temperature up to 500 °C. After annealing at 500 °C, the FWHM of the E_2 (high) mode is around 9 cm^{-1} similar to that found for this mode in single crystals (8 cm^{-1}) [21] thus indicating that the recrystallization process is almost finished.

4. Concluding remarks

The precedent results show that electrodeposition can be employed favourably to prepare partially oriented ZnO nanocolumnar thin films with a high crystal quality after thermal annealing at a temperature of 500 °C as attested by Raman scattering measurements. Interestingly, cathodic electrodeposition gives rise to a thin film constituted by hexagonal nanocolumns, but the as-grown crystals have a large amount of defects, i.e. are either fully amorphous or have a crystalline core and an amorphous wrapping (see spectra a and b). This heterogeneous structure has been suggested for ZnO nanostructures prepared by thermal evaporation. Annealing for 1 h in air induces an ordering and crystallization of the nanopillar monocrystals whose degree of crystallinity is higher, the higher the annealing temperature. In fact, the spectrum after heating at 500 °C evidences the high quality of the ZnO crystals.

Zinc oxide is considered as a promising material in UV photonics. It is therefore interesting to record photoluminescence spectra with the aim of correlating the degree of crystallinity as assessed through Raman spectra with the emission characteristics. Our electrodeposited ZnO nanostructures only showed significant emission in the UV range, with no visible emission related to defects. As the anneling temperature increases from 300 to 500 °C, the UV emission sharpens and shifts to the blue. This is interpreted as a diminution in non-radiative recombination centres, associated to defects, after annealing. This conclusion is perfectly compatible with Raman spectroscopy experiments.

Finally, from a practical point of view, it is remarkable that electrodeposition can be used as a simple, non-expensive method of synthesis of ZnO nanocolumnar films on conducting glass substrates. After annealing in air at moderate temperature (500 °C), nanocolumnar crystals of high quality are generated. These films, quite robust and adherent, also possess excellent emission in the ultraviolet, which confirms their possible use in UV photonic devices.

Acknowledgements

This work was supported through Spanish Government MCYT grant MAT2002-04539-C02-02 and the Universitat Politècnica de València (Programa d'Incentiu a la Recerca per a Projectes Interdisciplinars, project number 200206618). R.G. is grateful to the MCYT (through project BQU2003-03737) and to the SS.TT.II. of the Universitat d'Alacant.

References

[1] K. Tennakone, J. Bandara, P.K.M. Bandaranayake, G.R.A. Kumara, A. Konno, Jpn. J. Appl. Phys. 40 (2001) 732.

[2] F. Lenzmann, M. Nanu, O. Kijatkina, A. Belaidi, Thin Solid Films 451–452 (2004) 639.
[3] Y. Chen, D. Bagnall, T. Yao, Mater. Sci. Eng. B 75 (2000) 190.
[4] J. Cembrero, M. Perales, M. Mollar, B. Marí, Bol. Soc. Esp. Ceram. Vidrio 42 (2003) 379.
[5] B. Marí, M. Mollar, A. Mechkour, B. Hartiti, M. Perales, J. Cembrero, Microelectron. J. 35 (2004) 79.
[6] H.-J. Egelhaaf, D. Oelkrug, J. Cryst. Growth 161 (1996) 190.
[7] K. Vanheusen, C.H. Seager, W.L. Warren, D.R. Tallant, J.A. Voight, Appl. Phys. Lett. 68 (1996) 403.
[8] M.H. Huang, Y. Wu, H. Feick, N. Tran, E. Weber, P. Yang, Adv. Mater. 13 (2001) 113.
[9] K. Ip, M.E. Overberg, Y.W. Heo, D.P. Norton, S.J. Pearton, C.E. Stutz, B. Luo, F. Ren, D.C. Look, J.M. Zavada, Appl. Phys. Lett. 82 (2003) 385.
[10] D.C. Look, C. Coskun, B. Chaflin, G.C. Farlow, Physica B 340–342 (2003) 32.
[11] A. Segura, J.A. Sans, F.J. Manjón, A. Muñoz, M.J. Herrera-Cabrera, Appl. Phys. Lett. 83 (2003) 278.
[12] B. Marí, J. Cembrero, F.J. Manjón, M. Mollar, R. Gómez, in: Proceedings of the Fourth International Conference of Porous Semiconductor Science and Technology, Cullera, 2004, Phys. Stat. Sol. (c), in press.
[13] J. Serrano, A.H. Romero, F.J. Manjón, R. Lauck, M. Cardona, A. Rubio, Phys. Rev. B 69 (2004) 094306.
[14] M. Tzolov, N. Tzenov, D. Dimova-Malinovska, M. Kalitzova, C. Pizzuto, G. Vitali, G. Zollo, I. Ivanov, Thin Solid Films 379 (2000) 28.
[15] M. Tzolov, N. Tzenov, D. Dimova-Malinovska, M. Kalitzova, C. Pizzuto, G. Vitali, G. Zollo, I. Ivanov, Thin Solid Films 396 (2001) 274.
[16] T.C. Damen, S.P.S. Porto, B. Tell, Phys. Rev. 142 (1966) 570.
[17] C.A. Arguello, D.L. Rousseau, S.P.S. Porto, Phys. Rev. 181 (1969) 1351.
[18] J.M. Calleja, M. Cardona, Phys. Rev. B 16 (1977) 3753.
[19] F.J. Manjón, K. Syassen, R. Lauck, High Pressure Res. 22 (2002) 299.
[20] Y. Zhang, J.R. Wang, C. Chen, X. Luo, D. Yu, C. Lee, Appl. Phys. Lett. 83 (2003) 4631.
[21] J. Serrano, F.J. Manjón, A.H. Romero, F. Widulle, R. Lauck, M. Cardona, Phys. Rev. Lett. 90 (2003) 055510.